Autoresonant control of a pre-excited diocotron mode

V. V. Gorgadze
Physics Department, University of California, Berkeley, California 94720, USA

L. Friedland
Racah Institute of Physics, Hebrew University of Jerusalem, Jerusalem 91904, Israel

J. S. Wurtele
Physics Department, University of California, Berkeley, California 94720, USA

A new method for the manipulation of a pre-excited $l=1$ diocotron mode in a pure electron plasma in a Malmberg-Penning trap is proposed and analyzed. The plasma is passively coupled to an external oscillatory circuit with slowly varying parameters. A threshold on the coupling strength is derived beyond which the plasma is continuously self-phase-locked to the external circuit. In the case of a linearly chirped circuit frequency, this autoresonant plasma can be driven to the wall, and in the case of a chirped sinusoidal variation of the circuit frequency, the plasma can be driven to the center of the trap. Derived thresholds on the coupling strength are in good agreement with simulations. Unlike conventional feedback mechanisms, autoresonant phase locking is a consequence of the nonlinearity of the system. © *2007 American Institute of Physics.*
[DOI: 10.1063/1.2762131]

I. INTRODUCTION

Autoresonance in systems of coupled nonlinear waves and oscillations with slowly varying parameters has been recently investigated in a series of papers by Friedland and collaborators. (for recent developments in extended autoresonant systems, see Ref. [1]; a review of autoresonance in systems with a finite number of degrees of freedom can be found in Ref. [2]).

Generally, attempts to excite nonlinear systems by resonant, *constant* frequency perturbations are not efficient because the system saturates due to nonlinear dephasing. Nevertheless, under certain conditions, one can continuously exchange energy between different degrees of freedom in a nonlinear system by using *varying* frequency perturbations and slow passage through resonance, followed by a persistent nonlinear phase locking in the system, despite variation of the driving frequency. This phase locking results in a continuing excitation and comprises the essence of the autoresonance phenomenon. The phenomenon of autoresonance (termed "phase stability") was introduced by McMillan and Veksler.[3] Autoresonance is a widely applicable nonlinear phenomenon, appearing in relativistic particle accelerators,[4] atomic and molecular physics,[5] nonlinear dynamics,[6] and solar system dynamics.[7]

In this paper, we present and analyze a novel autoresonant scheme for controlling a *pre-excited* $l=1$ diocotron mode[8–10] in a Malmberg-Penning trap[11] by passive coupling to an external electric circuit with slowly varying parameters. In earlier studies,[12] the diocotron mode was autoresonantly controlled by applying an external oscillating perturbation of constant amplitude and slowly varying frequency. This method of excitation requires an initially zero amplitude mode, i.e., the plasma column must initially be at the center of the trap. Here, we demonstrate that a pre-excited dio-

cotron mode can be controlled by a different implementation of the autoresonant concept. This is achieved by coupling to a circuit, with its own time-varying resonant frequency, rather than to a chirped frequency drive. In the case that the circuit resonant frequency is varied linearly in time, we find that autoresonant coupling allows for the control of an excited diocotron mode. This does not work when the coupling is to the chirped external drive (since there is no route to adiabatically phase locking the drive and the diocotron mode). Here, the resonant circuit is initially unexcited, so that its phase can lock to that of the diocotron and the autoresonant coupling can then move the mode towards the wall. Finally, we present and analyze another variant of the autoresonant coupling scheme that involves an external circuit with a chirped, periodically modulated frequency. This application is related to resonant three-wave interactions and allows for manipulating the pre-excited plasma column to the center of the trap. This paper represents the first study of autoresonant coupling to an initially excited nonlinear system. As envisioned here, it is both a new method for the control of non-neutral plasmas and an example of how it can be used, potentially, to conduct experiments in nonlinear dynamics. To date, this method of control has not been used in non-neutral plasma experiments. Furthermore, the application here is autoresonant coupling to an initially excited dynamical system. Possible extensions can be envisioned to control pre-existing nonlinear waves, such as solitons and Bernstein-Green-Kruskal (BGK) modes.

This paper is organized as follows. Section II describes the autoresonant control of the diocotron mode via coupling to an external circuit with slowly varying parameters. We present our model and analyze the stages of resonant trapping and autoresonance synchronization. In particular, we derive the threshold for capture into autoresonance and study the subsequent dynamics. Section III extends the idea of con-
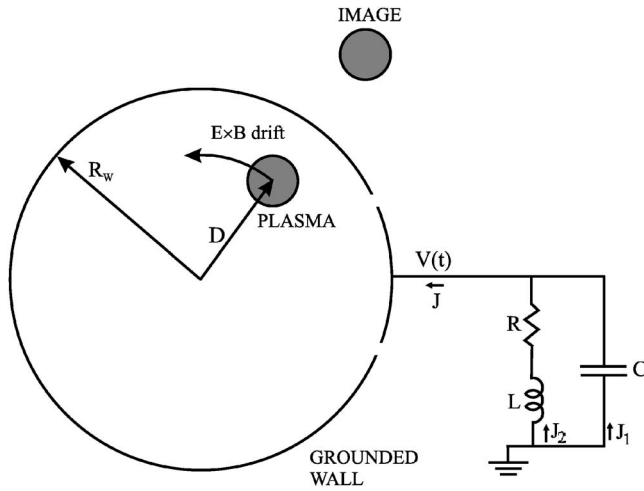
FIG. 1. Schematic of the system with an isolated sector on the trap wall connected to an external circuit. The circuit capacitance can be varied in time.

trol via coupling to a passive (without amplified feedback) external circuit by analyzing the use of chirped oscillating modulations of the external circuit. We present our conclusions in Sec. IV.

II. CONTROL OF THE DIOCOTRON MODE BY VARYING EXTERNAL CIRCUIT PARAMETERS

A. The model and dimensionless equations

Consider a magnetized plasma column in a cylindrical trap, as shown in Fig. 1. The dynamics of the column are assumed to be governed by the drift motion in the axial magnetic and radial electric fields. The latter is generated by image charges in the grounded conducting wall and the charges on the sector of the wall connected to the external LC circuit. This approach ignores end-field effects and the rotation of the column around its own axis. We treat the plasma as an axially infinite line of charge, and use polar coordinates (D, Θ) for the center-of-charge motion. The image line charge in an infinite grounded cylindrical wall has the opposite charge density and is located in the plane passing through the plasma column and the center of the trap. The image is located at the distance R_w^2/D from the center of the trap, where R_w is the wall radius. The resulting electric field inside the cylinder is discussed in the Appendix. The potential on the isolated driving sector will be determined later via Kirchoff equations.

Using Eq. (A6) for the electric field created by an external potential $V(t)$ and radial field from the image charge, one can write equations for the $E \times B$ drift motion of the plasma column,

$$\frac{dD}{dt} = \frac{E_\Theta}{B} = -\left.\frac{1}{Br}\frac{\partial \Phi}{\partial \phi}\right|_{r=D, \phi=\Theta}$$

$$= \frac{2V(t)}{\pi BD}\sum_{k=1}^{\infty}\left(\frac{D}{R_w}\right)^k \sin(k\Delta\theta)\sin(k\Theta), \quad (1)$$

$$\frac{d\Theta}{dt} = -\frac{E_r}{Br} = -\left.\frac{1}{Br}\frac{\partial \Phi}{\partial r}\right|_{r=D, \phi=\Theta}$$

$$= -\frac{\lambda}{2\pi\epsilon_0 B(R_w^2 - D^2)}$$

$$+ \frac{2V(t)}{\pi BDR_w}\sum_{k=1}^{\infty}\left(\frac{D}{R_w}\right)^{k-1}\sin(k\Delta\theta)\cos(k\Theta). \quad (2)$$

Here $\Phi(D, \Theta, t)$ is the total electric potential at the position of the plasma and $V(t)$ is the potential on the driving sector. These variables were used in previous models for autoresonant diocotron excitation.[12] As noted above, in the present work the plasma is coupled to an external circuit, thereby allowing autoresonant control of an initially excited mode. The circuit is connected to an azimuthal sector of the wall, as seen in Fig. 1. The charge on this sector couples to and drives the diocotron mode. Depending on the details of the circuit, we will see that the diocotron mode can be driven either towards the center of the cylinder or towards the wall.

Let Q be the charge on the driving sector, J_2 represent the current through the inductance L and resistor R, and $Q_2 = \int J_2 dt$. Then, the charge and the voltage on the circuit capacitor are $Q_C = Q - Q_2$ and $V(t) = -Q_C/C(t)$. Kirchoff's second law leads to

$$R\frac{dQ_2}{dt} + L\frac{d^2Q_2}{dt^2} = V(t) = \frac{Q_2 - Q}{C(t)}. \quad (3)$$

The charge on the driving sector can be written as $Q = Q_\lambda + C_{\text{eff}}V(t)$ [see Eq. (A5)], where Q_λ is given by Eq. (A4). This allows us to express the voltage on the sector as

$$V(t) = \frac{Q_2 - Q_\lambda}{C(t) + C_{\text{eff}}}. \quad (4)$$

Substitution of Eq. (4) into Eq. (3) yields an equation for Q_2,

$$\left(L\frac{d^2}{dt^2} + R\frac{d}{dt} + \frac{1}{C(t) + C_{\text{eff}}}\right)Q_2 = \frac{Q_\lambda}{C(t) + C_{\text{eff}}}. \quad (5)$$

A closed set of equations describing the system is reached by substituting Eq. (4) (for the potential on the sector) and Eq. (A4) into Eqs. (1) and (2),

$$\left(L\frac{d^2}{dt^2} + R\frac{d}{dt} + \frac{1}{C(t) + C_{\text{eff}}}\right)Q_2$$

$$= -\frac{l\lambda}{\pi[C(t) + C_{\text{eff}}]}$$

$$\times \left(\Delta\theta + \sum_{k=1}^{\infty}\left(\frac{D}{R_w}\right)^k\frac{2\cos(k\Theta)\sin(k\Delta\theta)}{k}\right), \quad (6)$$

$$\frac{dD}{dt} = \frac{2}{\pi BD[C(t) + C_{\text{eff}}]}$$
$$\times \left\{ Q_2 + \frac{l\lambda}{\pi}\left[\Delta\theta + \sum_{k=1}^{\infty}\left(\frac{D}{R_w}\right)^k \right.\right.$$
$$\left.\left. \times\frac{2\cos(k\Theta)\sin(k\Delta\theta)}{k} \right] \right\}$$
$$\times \sum_{k=1}^{\infty}\left(\frac{D}{R_w}\right)^k \sin(k\Delta\theta)\sin(k\Theta), \tag{7}$$

$$\frac{d\Theta}{dt} = -\frac{\lambda}{2\pi\epsilon_0 B(R_w^2 - D^2)} + \frac{2}{\pi BDR_w(C(t) + C_{\text{eff}})}$$
$$\times \left\{ Q_2 + \frac{l\lambda}{\pi}\left[\Delta\theta + \sum_{k=1}^{\infty}\left(\frac{D}{R_w}\right)^k \right.\right.$$
$$\left.\left. \times\frac{2\cos(k\Theta)\sin(k\Delta\theta)}{k} \right] \right\}$$
$$\times \sum_{k=1}^{\infty}\left(\frac{D}{R_w}\right)^{k-1} \sin(k\Delta\theta)\cos(k\Theta). \tag{8}$$

Here $2\Delta\theta$ is the angular width of the driving sector. In studying autoresonance at the fundamental frequency, we ignore all nonresonant terms, referring to the resonance condition, Eq. (12), below. Thus, keeping $k=1$ terms only, we have

$$\left(L\frac{d^2}{dt^2} + R\frac{d}{dt} + \frac{1}{C(t) + C_{\text{eff}}} \right)Q_2$$
$$= -\frac{l\lambda}{\pi[C(t) + C_{\text{eff}}]}\frac{2D}{R_w}\sin(\Delta\theta)\cos\Theta, \tag{9}$$

$$\frac{dD}{dt} = \frac{Q_2}{\pi BD[C(t) + C_{\text{eff}}]}\frac{2D}{R_w}\sin(\Delta\theta)\sin\Theta, \tag{10}$$

$$\frac{d\Theta}{dt} = -\frac{\lambda}{2\pi\epsilon_0 B(R_w^2 - D^2)} + \frac{2Q_2\sin(\Delta\theta)\cos\Theta}{\pi BDR_w[C(t) + C_{\text{eff}}]}. \tag{11}$$

The initial stage of autoresonance involves passage through resonance by slow variation of the frequency of the LC circuit. We chirp through the diocotron frequency at the initial position D_0 of the column and assuming, for simplicity, a linear frequency chirp,

$$\frac{1}{\sqrt{L(C(t) + C_{\text{eff}})}} = -\frac{\lambda}{2\pi\epsilon_0 B(R_w^2 - D_0^2)} + At, \tag{12}$$

where A is the chirp rate. We change to the normalized action $I_1 \equiv D^2/R_w^2$, and define $I_{10} = D_0^2/R_w^2$. We define the dimensionless time $\tau = \Omega_d t$, frequency $\Omega(t) = \sqrt{1/\{L[C(t) + C_{\text{eff}}]\}}/\Omega_d$, chirp rate $\alpha = A/\Omega_d^2$, circuit dissipation $\nu = (4\pi\epsilon_0 BR_w^2/2|\lambda|L)R$, and charge $q = Q_2\sqrt{L/2\pi\epsilon_0 B^2 lR_w^4}$. The diocotron frequency $\Omega_d \equiv |\lambda|/2\pi\epsilon_0 BR_w^2$. We introduce the dimensionless coupling parameter as

$$\epsilon = \sqrt{\frac{2\lambda^2 Ll\sin^2(\Delta\theta)}{\pi^3\epsilon_0 B^2 R_w^4}}. \tag{13}$$

In these dimensionless variables, Eqs. (9)–(11) become

$$\left[\frac{d^2}{d\tau^2} + \nu\frac{d}{d\tau} + \Omega^2(\tau) \right]q = \epsilon\Omega^2(\tau)\sqrt{I_1}\cos\Theta, \tag{14}$$

$$\frac{dI_1}{d\tau} = 2\epsilon\Omega^2(\tau)\sqrt{I_1}q\sin\Theta, \tag{15}$$

$$\frac{d\Theta}{d\tau} = \frac{1}{1 - I_1} + \epsilon\frac{\Omega^2(\tau)q\cos\Theta}{\sqrt{I_1}}, \tag{16}$$

where the chirped circuit frequency can be expressed as, using Eq. (12),

$$\Omega(\tau) = \frac{1}{1 - I_{10}} + \alpha\tau,$$

passing through resonance at $\tau = 0$. We solve this system subject to the initial conditions

$$I_1(\tau \rightarrow -\infty) = I_{10}, \tag{17}$$

$$q(\tau \rightarrow -\infty) = 0, \tag{18}$$

$$\frac{dq}{d\tau}(\tau \rightarrow -\infty) = 0. \tag{19}$$

B. Autoresonant evolution

The coupled nonlinear system of Eqs. (14)–(16) permits different classes of solutions. The analysis proceeds by extending the analysis of autoresonance in Ref. 12 to include coupling to an external circuit. The analysis is simplified by assuming that the circuit has a high-quality factor and neglecting the dissipation ($R=0$). This assumption is discussed at the end of this section. Next, we use a two-scale representation of the solution

$$q(\tau) = a(\tau)e^{i\Theta_2(\tau)} + \text{c.c.},$$

where the amplitude is assumed to be a slow variable, while phase Θ_2 is fast, but frequency $\dot\Theta_2$ is a slow variable. We substitute this representation into Eq. (14), yielding

$$(2i\dot a\dot\Theta_2 + i\ddot\Theta_2 a - \dot\Theta_2^2 a + \Omega^2 a)e^{i\Theta_2(\tau)} = (\epsilon/2)\Omega^2(\tau)\sqrt{I_1}e^{i\Theta(\tau)}. \tag{20}$$

Then, separating the real and imaginary parts, we obtain

$$2\dot a\dot\Theta_2 + \ddot\Theta_2 a = \frac{\epsilon}{2}\Omega^2(\tau)\sqrt{I_1}\sin(\Theta - \Theta_2), \tag{21}$$

$$(\Omega^2 - \dot\Theta_2^2)a = \frac{\epsilon}{2}\Omega^2(\tau)\sqrt{I_1}\cos(\Theta - \Theta_2). \tag{22}$$

We shall see later that, in autoresonance, phase mismatch $\Phi = \Theta - \Theta_2$ in the last equations performs slow, small

amplitude oscillations around a slowly varying average. In other words, $\dot{\Theta} \approx \dot{\Theta}_2 \approx \Omega$. A new action variable, $I_2 = a^2 \dot{\Theta}_2$, simplifies the system to

$$\dot{I}_2 = \frac{\epsilon}{2}\Omega^{3/2}(\tau)\sqrt{I_1 I_2}\,\sin\Phi, \tag{23}$$

$$\dot{\Theta}_2 = \Omega - \frac{\epsilon}{4}\Omega^{3/2}(\tau)\sqrt{\frac{I_1}{I_2}}\,\sin\Phi. \tag{24}$$

The equations of motion of the plasma column, Eqs. (15) and (16), should be simplified as well. We substitute $q = 2a\cos\Theta_2$ and eliminate all nonresonant terms on the right-hand side (RHS) of Eqs. (15) and (16) leaving only terms varying as $\sim e^{i\Phi}$,

$$\dot{I}_1 = 2\epsilon\Omega^{3/2}(\tau)\sqrt{I_1 I_2}\,\sin\Phi, \tag{25}$$

$$\dot{\Theta} = \frac{1}{1-I_1} + \epsilon\Omega^{3/2}(\tau)\sqrt{\frac{I_2}{I_1}}\,\cos\Phi. \tag{26}$$

Equations (23) and (25) satisfy the conservation law

$$I_1 - 4I_2 = I_{10}.$$

Note that both actions are positive. Therefore, starting with an initially unexcited circuit, which is necessary for capturing all initial phases in resonance, a current is induced in the circuit and both actions I_1 and I_2 increase. Thus, this approach does not allow driving of the mode towards the center of the trap (i.e., the decrease of action I_1). This will be further discussed in Sec. III. The conservation of $I_1 - 4I_2$ yields the desired reduced system for the action I_2 and the phase mismatch Φ,

$$\dot{I}_2 = \frac{\epsilon}{2}\Omega^{3/2}(\tau)\sqrt{(I_{10}+4I_2)I_2}\,\sin\Phi, \tag{27}$$

$$\dot{\Phi} = \frac{1}{1-I_{10}-4I_2} - \Omega + \epsilon\Omega^{3/2}(\tau)$$
$$\times\left(\frac{1}{4}\sqrt{\frac{I_{10}+4I_2}{I_2}} + \sqrt{\frac{I_2}{I_{10}+4I_2}}\right)\cos\Phi. \tag{28}$$

At the initial stage of evolution, I_2 remains small compared to the excited action I_1, so one can neglect I_2 in the RHS of Eqs. (27) and (28) at this stage, yielding

$$\dot{I}_2 = \frac{\epsilon\Omega^{3/2}(\tau)\sqrt{I_{10}}}{2}\sqrt{I_2}\,\sin\Phi, \tag{29}$$

$$\dot{\Phi} = \frac{1}{1-I_{10}-4I_2} - \frac{1}{1-I_{10}} - \alpha\tau$$
$$+ \frac{\epsilon\Omega^{3/2}(\tau)\sqrt{I_{10}}}{4}\frac{1}{\sqrt{I_2}}\cos\Phi. \tag{30}$$

We linearize the first term in Eq. (30), define new coupling and nonlinear frequency shift parameters

$$\tilde{\epsilon} = \frac{\epsilon\Omega^{3/2}(\tau)\sqrt{I_{10}}}{4}, \tag{31}$$

$$\beta = \frac{4}{(1-I_{10})^2}, \tag{32}$$

and rewrite Eqs. (29) and (30) in the simplified form

$$\dot{I}_2 = 2\tilde{\epsilon}\sqrt{I_2}\,\sin\Phi, \tag{33}$$

$$\dot{\Phi} = \beta I_2 - \alpha\tau + \frac{\tilde{\epsilon}}{\sqrt{I_2}}\cos\Phi. \tag{34}$$

With the exception of slow time dependence of $\tilde{\epsilon}$, we have reduced our system to one that is similar to that studied in Ref. 12. This time dependence of $\tilde{\epsilon}$ is shown below not to effect autoresonant phase locking.

Further analysis is required to arrive at a threshold for autoresonance. We set $I_2 = I_2^{(0)} + \Delta$, where $I_2^{(0)}(\tau)$ is a slow, monotonically varying function of time and $\Delta(\tau)$ is a small oscillation, and seek a phase-locked solution, i.e., $\Phi = \pi + \tilde{\Phi}$, where $|\tilde{\Phi}| \ll \pi$. With these substitutions, linearizing Eq. (34) yields

$$\dot{\tilde{\Phi}} = \left(\beta + \frac{\tilde{\epsilon}}{2(I_2^{(0)})^{3/2}}\right)\Delta - \alpha t + \beta I_2^{(0)} - \frac{\tilde{\epsilon}}{\sqrt{I_2^{(0)}}}\cos\tilde{\Phi}. \tag{35}$$

Now define the slow function $I_2^{(0)}(\tau)$ that satisfies

$$-\alpha\tau + \beta I_2^{(0)}(\tau) - \frac{\tilde{\epsilon}(\tau)}{\sqrt{I_2^{(0)}(\tau)}} \equiv 0. \tag{36}$$

The phase evolution becomes

$$\dot{\tilde{\Phi}} = S\Delta, \tag{37}$$

where $S \equiv \beta + (\tilde{\epsilon}/2)[I_2^{(0)}]^{-3/2}$ is slowly varying. The differentiation of Eq. (36) yields

$$\dot{I}_2^{(0)} = \frac{\alpha}{S}\left(1 + \frac{3\tilde{\epsilon}}{2\Omega\sqrt{I_2^{(0)}}}\right). \tag{38}$$

Note that the second term in the bracket in Eq. (38) enters due to the time dependence of $\tilde{\epsilon}$, in contrast to the case considered in Ref. 12, where the coupling parameter ϵ was time independent. Finally, we find the lowest-order equation for $\dot{\Delta}$,

$$\dot{\Delta} = \dot{I}_2 - \dot{I}_2^{(0)} = -2\tilde{\epsilon}I_2^{(0)1/2}\sin\tilde{\Phi} - \frac{\alpha}{S}\left(1 + \frac{3\tilde{\epsilon}}{2\Omega\sqrt{I_2^{(0)}}}\right). \tag{39}$$

Equations (37) and (39) comprise a Hamiltonian system with Hamiltonian

$$H(\tilde{\Phi},\Delta) = \frac{S\Delta^2}{2} + V_{\text{eff}}(\tilde{\Phi}),$$

and effective tilted cosine potential

$$V_{\text{eff}}(\tilde{\Phi}) = -2\tilde{\epsilon}I_2^{(0)1/2}\cos\tilde{\Phi} + \tilde{\Phi}\frac{\alpha}{S}\left(1 + \frac{3\tilde{\epsilon}}{2\Omega\sqrt{I_2^{(0)}}}\right).$$

The problem thus reduces to that of a pseudoparticle of slowly varying mass S^{-1} moving in a slowly varying V_{eff}. A pseudoparticle remains trapped, under adiabatic conditions, as long as potential wells exist in V_{eff}. Whenever
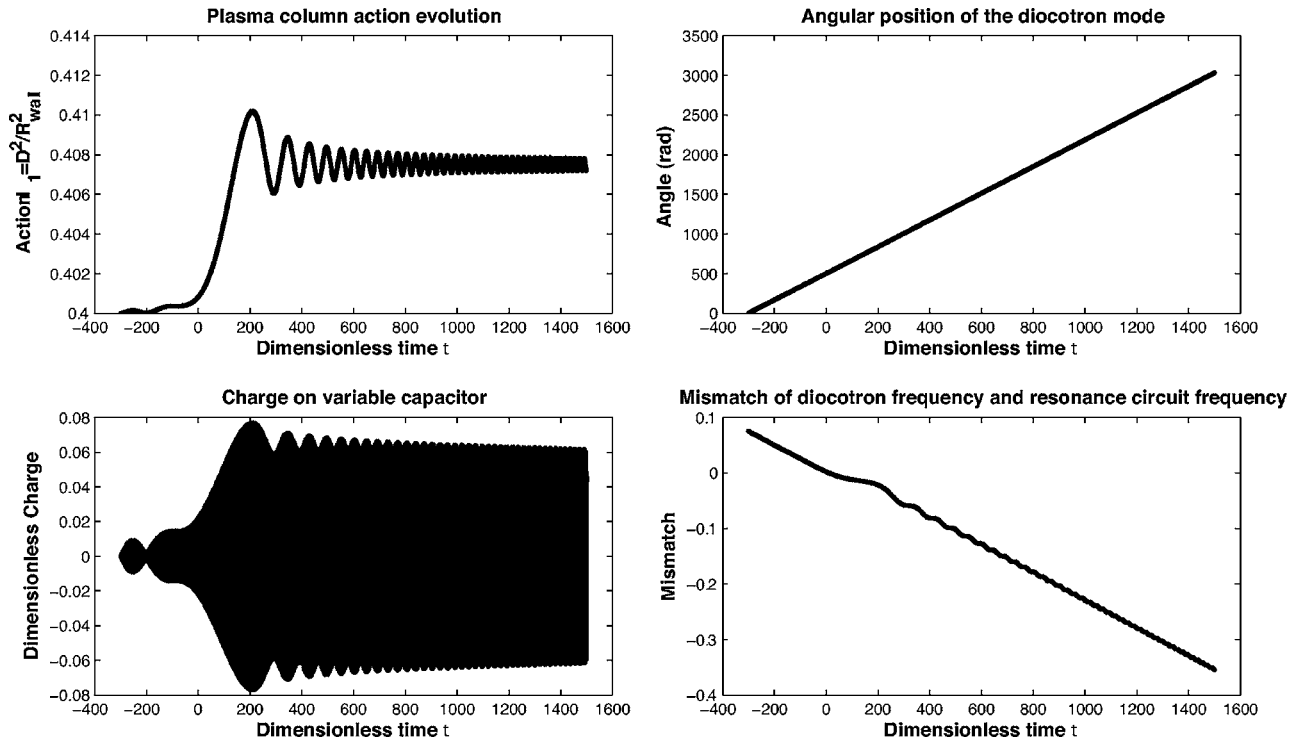
FIG. 2. The numerical solution of Eqs. (14)–(16) for coupling parameter ϵ below the threshold. The diocotron mode action increases by just 2% as the system passes through resonance.

$$\frac{dV_{\text{eff}}}{d\tilde{\Phi}} > 0,$$

for all $\tilde{\Phi}$, or,

$$\alpha > \frac{2\tilde{\epsilon}\sqrt{I_2^{(0)}}S}{1 + \frac{3\tilde{\epsilon}}{2\Omega\sqrt{I_2^{(0)}}}}, \tag{40}$$

potential wells cease to exist. The RHS of Eq. (40) depends on $I_2^{(0)}$ both directly and through the "mass" S. A phase-locked solution requires that the chirp rate α does not exceed the minimum value of the RHS of Eq. (40). We differentiate the RHS of Eq. (40) to find the value of the action at the minimum. Neglecting the second term in the denominator (this term scales as $\tilde{\epsilon}^{2/3} \ll 1$; see below), the minimum action $I_{2,\min}^{(0)} = (\tilde{\epsilon}/\beta)^{2/3} \sim \tilde{\epsilon}^{2/3}$. Then, the coupling parameter must satisfy

$$\tilde{\epsilon} > (\alpha/3)^{3/4}\beta^{-1/2}. \tag{41}$$

Thus, to lowest order in the small parameter $\tilde{\epsilon}$, the neglected term in the denominator of the RHS of Eq. (40) scales as $\tilde{\epsilon}^{2/3} \ll 1$. Recall that this term in the denominator is a consequence of time dependence of the driving parameter $\tilde{\epsilon}$. Consequently, this slow time dependence can be ignored. Conditions in Eq. (41) should be expressed in terms of our original parameters, yielding an autoresonance threshold condition on the coupling parameter,

$$\epsilon > \epsilon_{th} = \frac{2}{3^{3/4}}(1 - I_{10})^{5/2}\Gamma_{10}^{1/2}\alpha^{3/4}. \tag{42}$$

We test these results by solving the system of Eqs. (14)–(16) numerically. We proceed by neglecting dissipation in these calculations. We start with an unexcited circuit with a chirped frequency (initially below the diocotron resonance) and an excited diocotron mode at $I_{10}=0.4$. We slowly chirp through the resonance, at the chirp rate $\alpha = 2.5 \times 10^{-4}$. Figure 2 shows simulation results for $\epsilon = 6.5 \times 10^{-4}$, i.e., below threshold ($\epsilon_{th}=7.7 \times 10^{-4}$). Rapid dephasing occurs after passage through resonance, resulting in very small perturbations of the diocotron mode and induced charge on the capacitor.

The behavior of the solution changes dramatically when the coupling parameter is increased above the threshold. This is demonstrated in Fig. 3, which shows the numerical solution of Eqs. (14)–(16) for identical initial conditions and parameters as in Fig. 2, except that now $\epsilon = 8.0 \times 10^{-4}$. As expected, the phase mismatch Φ locks near π, the system remains in autoresonance, and the continuing weak coupling to the circuit produces a large change in the diocotron mode, driving it towards the wall. The range of validity of our analytical expression for the threshold is illustrated in Fig. 4, where we plot theoretical estimates and simulation results for the coupling parameter threshold as a function of the chirp rate α.

Finally, we include dissipation. The quality factor of the circuit is related to dimensionless resistance ν by

$$Q = \frac{\Omega_{\text{circuit}}L}{R} \approx \frac{1}{\nu(1 - I_{10})}.$$

We numerically found a linear dependence of ϵ_{th} on ν. This is consistent with earlier results on dissipation in exter-
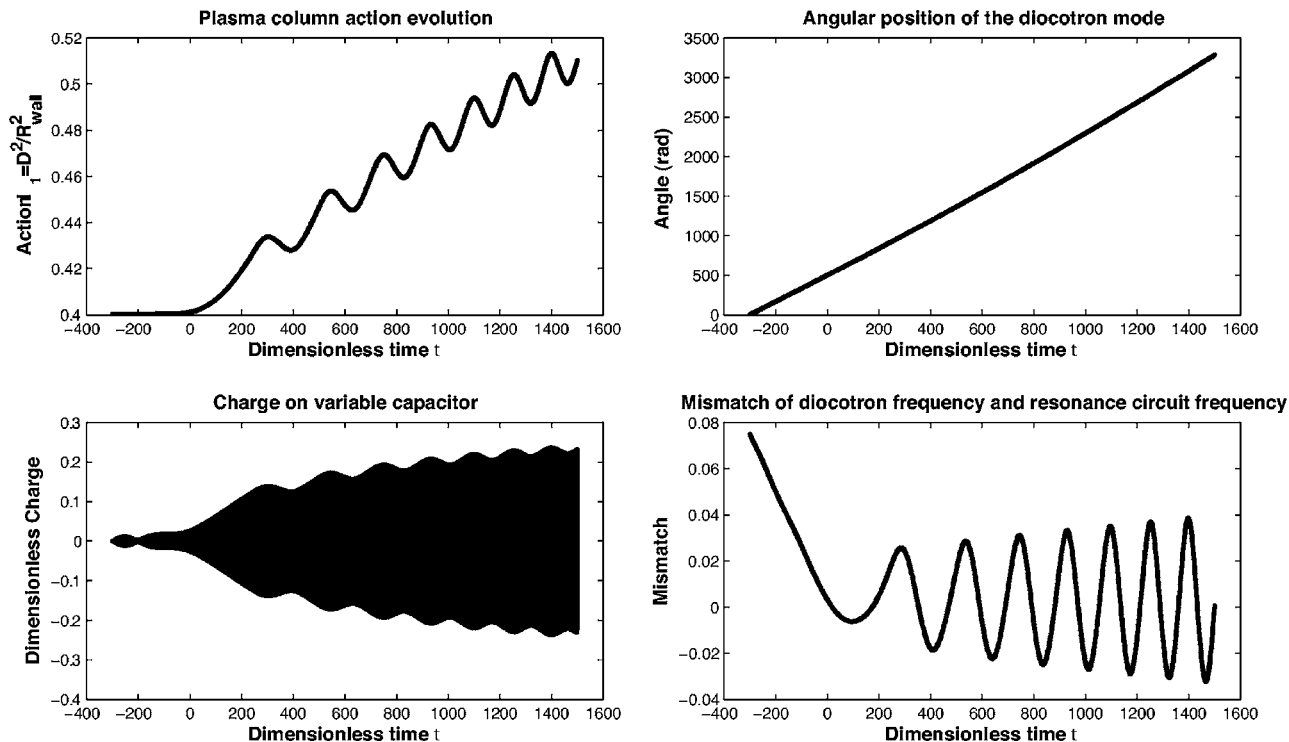
FIG. 3. The numerical solution of Eqs. (14)–(16) when the coupling parameter ϵ is just above ϵ_{th}. The diocotron mode action increases continuously. The frequency of the diocotron mode, on average, follows the chirped frequency of the circuit.

nally driven diocotron modes [see Eq. (15) in Ref. 13]. Simulations show that a change in the threshold of 10% requires a quality factor $Q \sim 200$. For larger Q, the dissipation has a smaller effect on the threshold, and, hence, the assumption of $\nu = 0$ in the theory remains very good for a wide range of realizable electrical circuits.

III. AUTORESONANCE WITH AN OSCILLATING MODULATION OF AN EXTERNAL CIRCUIT

Our method for control of the diocotron mode with a linearly chirped frequency in the external circuit, as given in Eq. (12), can be used to drive a pre-excited diocotron mode
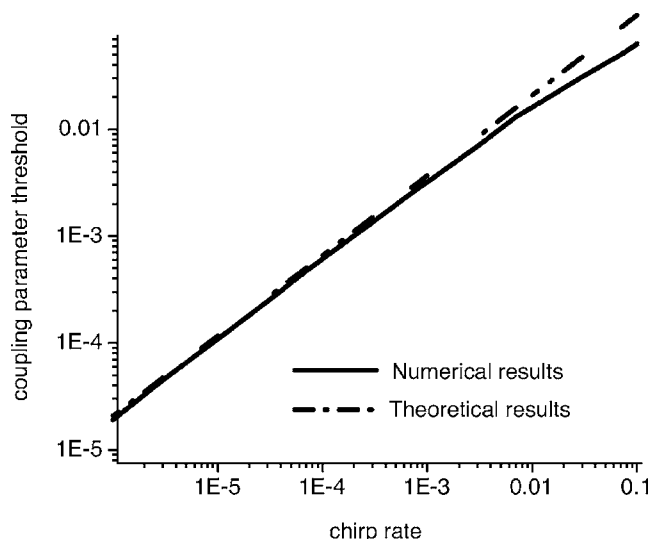

FIG. 4. Comparison of the theoretical estimate of the coupling parameter $\epsilon_t h$ threshold from Eq. (42) (dot-dashed line) and simulation results (straight line) for the threshold for various chirp rates α.

towards the wall. It cannot drive the mode to the axis. We show here that a chirped sinusoidal frequency modulation of the external circuit inductance can autoresonantly drive the plasma to the center of the trap. Let

$$L(t) = L_0[1 + \delta \cos \psi(t)],$$

where $\delta \ll 1$ and rate of change of $\psi(t)$ is chirped through a frequency ω_ψ^0 (to be defined later),

$$\frac{d\psi(t)}{dt} = \omega_\psi(t) = \omega_\psi^0 + At.$$

The time dependence of the inductance $L(t)$ leads to a modification of Kirchoff's equation through the replacement $L(d^2Q_2/dt^2) \rightarrow (d/dt)[L(t)(d/dt)Q_2]$, and the evolution of the charge Q_2 [compare with Eq. (5)] is governed by

$$\left[L\frac{d^2}{dt^2} + \frac{dL(t)}{dt}\frac{d}{dt} + R\frac{d}{dt} + \frac{1}{C + C_{\text{eff}}} \right] Q_2 = \frac{Q_\lambda}{C + C_{\text{eff}}}. \quad (43)$$

Following the development in Sec. II A, we expand Q_λ on the RHS of Eq. (43) and keep the resonant terms in Eq. (43) and in the drift equations. This yields

$$\frac{dD}{dt} = \frac{Q_2}{\pi BD(C + C_{\text{eff}})}\frac{2D}{R_w}\sin(\Delta\theta)\sin(\Theta), \quad (44)$$

$$\frac{d\Theta}{dt} = -\frac{2\lambda}{4\pi\epsilon_0 B(R_w^2 - D^2)} + \frac{2Q_2\sin(\Delta\theta)\cos(\Theta)}{\pi BDR_w(C + C_{\text{eff}})}, \quad (45)$$

$$\left[L\frac{d^2}{dt^2} + \frac{dL(t)}{dt}\frac{d}{dt} + R\frac{d}{dt} + \frac{1}{C + C_{\text{eff}}}\right]Q_2$$
$$= -\frac{l\lambda}{\pi(C + C_{\text{eff}})}\frac{2D}{R_w}\sin(\Delta\theta)\cos(\Theta), \tag{46}$$

$$\frac{dL(t)}{dt} = -L_0\delta(\omega_\psi^0 + At)\sin\psi(t). \tag{47}$$

Next, define the dimensionless modulation frequency $\Omega_\psi = \Omega_d^{-1}\omega_\psi$, while other dimensionless parameters are the same as have been introduced in Sec. II A. Then, Eqs. (44)–(46) become

$$\left[(1 + \delta\cos\Psi)\frac{d^2}{d\tau^2} - \Omega_\psi\delta\sin\Psi\frac{d}{d\tau} + \nu\frac{d}{d\tau} + \Omega_c^2\right]q$$
$$= \tilde{\epsilon}\sqrt{I_1}\cos\Theta, \tag{48}$$

$$\frac{dI_1}{d\tau} = 2\tilde{\epsilon}\sqrt{I_1}q\sin\Theta, \tag{49}$$

$$\frac{d\Theta}{d\tau} = \frac{1}{1 - I_1} + \tilde{\epsilon}\frac{q\cos\Theta}{\sqrt{I_1}}, \tag{50}$$

where $\tilde{\epsilon} = \Omega_c^2\epsilon$ and

$$\frac{d\Psi}{d\tau} = \Omega_\psi(\tau) = \Omega_\psi^0 + \alpha\tau.$$

The initial conditions here are as in Eqs. (17) and (18) above, and we take $\nu = 0$. There exist three slowly varying frequencies in the system: the diocotron mode frequency, the circuit resonant frequency, and the frequency of modulation of the inductance. We seek three-wave resonances that meet the condition (we keep both signs for now; later we will consider them separately)

$$\dot{\Theta} - \dot{\Psi} \approx \mp\dot{\Theta}_c.$$

Our analysis proceeds by assuming small $\tilde{\epsilon} \ll 1$ and $\delta \ll 1$. In the limit $\delta = \tilde{\epsilon} = 0$, $q(t)$ oscillates with frequency Ω_c. Terms with $\delta\cos\psi(t)$ or $\delta\sin\psi(t)$ lead to aperiodic solutions containing linear combinations of the two main frequencies, Ω_c and Ω_ψ. We avoid additional resonances by assuming that these frequencies are not commensurate.

We seek solutions of form

$$q(\tau) = a(\tau)e^{i\Theta_c(\tau)} + b(\tau)e^{i[\Theta_c(\tau)\mp\Psi(\tau)]} + c(\tau)e^{i\Theta(\tau)} + \text{c.c.},$$

substitute $q(\tau)$ into Eq. (48), and separate terms corresponding to different frequencies. We neglect time derivatives of the slowly varying (small) nonresonant envelopes $b(\tau)$ and $c(\tau)$.

Both the RHS and left-hand side (LHS) of Eq. (48) have terms oscillating as $e^{i\Theta(\tau)}$, yielding

$$c = \frac{\tilde{\epsilon}}{2(\Omega_c^2 - \dot{\Theta}^2)}\sqrt{I_1}.$$

Next, consider the nonresonant terms varying as $e^{i[\Theta_c(\tau)\mp\Psi(\tau)]}$. The RHS of Eq. (48) yields zero, and the LHS yields

$$[-(\dot{\Theta}_c \mp \dot{\Psi})^2 + \Omega_c^2]be^{i(\Theta_c(\tau)\mp\Psi(\tau))}$$
$$+ \frac{\delta}{2}\frac{d}{d\tau}[ia\dot{\Theta}_c e^{i(\Theta_c(\tau)\mp\Psi(\tau))}] + \text{c.c.} = 0. \tag{51}$$

Solving for $b(\tau)$, we obtain $[-(\dot{\Theta}_c \mp \dot{\Psi})^2 + \Omega_c^2]b = (\delta/2)a\dot{\Theta}_c(\dot{\Theta}_c \mp \dot{\Psi})$ or

$$b = \delta\frac{\Omega_c^{1/2}(\dot{\Theta}_c \mp \dot{\Psi})}{2[\Omega_c^2 - (\dot{\Theta}_c \mp \dot{\Psi})^2]}\sqrt{I_2}, \tag{52}$$

where $I_2 = a^2\dot{\Theta}_c$, and we used $\dot{\Theta}_c \approx \Omega_c$, as justified by Eq. (57) below. Finally, we focus on the main oscillation, having phase factor $e^{i\Theta_c(\tau)}$,

$$[2i\dot{a}\dot{\Theta}_c + ia\ddot{\Theta}_c - a\dot{\Theta}_c^2 + a\Omega_c^2]e^{i\Theta_c(\tau)}$$
$$+ \frac{\delta}{2}\frac{d}{dt}[ic\dot{\Theta}e^{i(\Theta(\tau)-\Psi(\tau))}] + \text{c.c.} = 0. \tag{53}$$

Assuming that, in autoresonance, the phase mismatch

$$\Phi(\tau) = \Theta(\tau) - \Psi(\tau) \pm \Theta_c(\tau)$$

varies slowly with respect to the fast phases, $|\dot{\Phi}| \ll \dot{\Psi}, \dot{\Theta}, \dot{\Theta}_c$, we rewrite Eq. (53) as

$$[2i\dot{a}\dot{\Theta}_c + ia\ddot{\Theta}_c - a\dot{\Theta}_c^2 + a\Omega_c^2] = \mp\frac{\delta}{2}c\dot{\Theta}\dot{\Theta}_c e^{\mp i\Phi}.$$

This, after separating real and imaginary parts, yields

$$2\dot{a}\dot{\Theta}_c + a\ddot{\Theta}_c = \frac{\delta}{2}c\dot{\Theta}\dot{\Theta}_c\sin\Phi, \tag{54}$$

$$(\Omega_c^2 - \dot{\Theta}_c^2)a = \mp\frac{\delta}{2}c\dot{\Theta}\dot{\Theta}_c\cos\Phi. \tag{55}$$

Using $I_2 = a^2\dot{\Theta}_c$ and $\dot{\Theta}_c \approx \Omega_c$ gives

$$\frac{dI_2}{d\tau} = \frac{\tilde{\epsilon}\delta}{4}\frac{\dot{\Theta}\sqrt{I_1\Omega_c}}{(\Omega_c^2 - \dot{\Theta}^2)}\sqrt{I_2}\sin\Phi, \tag{56}$$

$$\frac{d\Theta_c}{d\tau} = \Omega_c \pm \frac{\tilde{\epsilon}\delta}{4}\frac{\dot{\Theta}\sqrt{I_1\Omega_c}}{(\Omega_c^2 - \dot{\Theta}^2)}\frac{\cos\Phi}{2\sqrt{I_2}}. \tag{57}$$

Finally, we substitute the ansatz for $q(\tau)$ into Eqs. (49) and (50). Only the resonant terms [such as $be^{i(\Theta_c\mp\Psi)} = be^{\pm i(\Phi-\Theta)}$ and $ce^{i\Theta}$] are retained, resulting in

$$\frac{dI_1}{d\tau} = 2\tilde{\epsilon}I_1^{1/2}b\sin\Phi$$
$$= \tilde{\epsilon}\delta\frac{\sqrt{I_1\Omega_c}(\dot{\Theta}_c \mp \dot{\Psi})}{\Omega_c^2 - (\dot{\Theta}_c \mp \dot{\Psi})^2}\sqrt{I_2}\sin\Phi$$
$$\approx \mp\tilde{\epsilon}\delta\frac{\dot{\Theta}\sqrt{I_1\Omega_c}}{\Omega_c^2 - \dot{\Theta}^2}I_2^{1/2}\sin\Phi, \tag{58}$$

$$\frac{d\Theta}{d\tau} = \frac{1}{1-I_1} + \frac{\widetilde{\epsilon}[c + b\cos\Phi]}{\sqrt{I_1}}$$

$$= \frac{1}{1-I_1} + \frac{\widetilde{\epsilon}}{\sqrt{I_1}}\left[\frac{\widetilde{\epsilon}}{\sqrt{I_1}}2(\Omega_c^2 - \dot{\Theta}^2)\right.$$

$$\left. + \frac{\delta\sqrt{\Omega_c}(\dot{\Theta}_c \mp \dot{\Psi})\sqrt{I_2}}{2[\Omega_c^2 - (\dot{\Theta}_c \mp \dot{\Psi})^2]}\cos\Phi\right]. \tag{59}$$

Equations (56) and (58) yield the conservation law

$$I_1 \pm 4I_2 = I_0. \tag{60}$$

Thus, in the case $I_1 - 4I_2 = I_0$, autoresonance in the system excites the diocotron mode and moves the plasma towards the wall. However, when $I_1 + 4I_2 = I_0$, the mode can be autoresonantly de-excited, and the plasma moves towards the axis of the trap. This is made clear in the following analysis.

By combining Eqs. (57) and (59), we find

$$\dot{\Phi} = \dot{\Theta} - \dot{\Psi} \pm \dot{\Theta}_c$$

$$= \left(\frac{1}{1-I_1} + \frac{\widetilde{\epsilon}^2}{2(\Omega_c^2 - \dot{\Theta}^2)} \pm \Omega_c - \Omega_\Psi^0\right) - \alpha\tau$$

$$+ \frac{\widetilde{\epsilon}\delta}{4}\frac{\Omega_c^{1/2}\dot{\Theta}}{(\Omega_c^2 - \dot{\Theta}^2)}\left(\frac{1}{2}\sqrt{\frac{I_1}{I_2}} \pm 2\sqrt{\frac{I_2}{I_1}}\right)\cos\Phi. \tag{61}$$

The analogy with the case studied in Sec. II A [compare with Eq. (34)] is made clear if we choose Ω_Ψ^0 so that the term in parentheses in the first line of Eq. (61) vanishes at $\tau = 0$,

$$\Omega_\Psi^0 = \frac{1}{1-I_{10}} + \frac{\widetilde{\epsilon}^2(1-I_{10})^2}{(\Omega_c^2(1-I_{10})^2 - 1)} \pm \Omega_c.$$

Next, we linearize $1/(1-I_1)$, use Eq. (60), and assume $I_2 \ll I_1$ (valid at the initial excitation stage) and $\dot{\Theta} \approx 1/(1-I_{10})$. This yields

$$\dot{\Phi} = \mp\beta I_2 - \alpha\tau + \gamma\frac{\cos\Phi}{\sqrt{I_2}}, \tag{62}$$

where β is defined in Eq. (32) and

$$\gamma = \frac{\widetilde{\epsilon}\delta}{8}\frac{\sqrt{I_{10}\Omega_c}(1-I_{10})}{(\Omega_c^2(1-I_{10})^2 - 1)}.$$

We rewrite Eq. (56) using this definition of γ,

$$\dot{I}_2 = 2\gamma\sqrt{I_2}\sin\Phi. \tag{63}$$

Equations (62) and (63) are characteristic equations of autoresonance, as described in Sec. II A. The lower sign in Eqs. (60) and (62) corresponds to the case analyzed in Sec. II B. The chirp rate threshold is again found from the autoresonance condition $\gamma > (|\alpha|/3)^{3/4}/\sqrt{\beta}$; converting into the parameters used in Eqs. (48)–(50) yields

$$|\alpha|^{3/4} < \epsilon\delta\frac{3^{3/4}\Omega_c^{5/2}I_{10}^{1/2}}{4|\Omega_c^2(1-I_{10})^2 - 1|}. \tag{64}$$

We have tested these results by solving Eqs. (48)–(50) numerically. As an example, we take $\Omega_c = 3.2$, $\alpha = -10^{-4}$, and
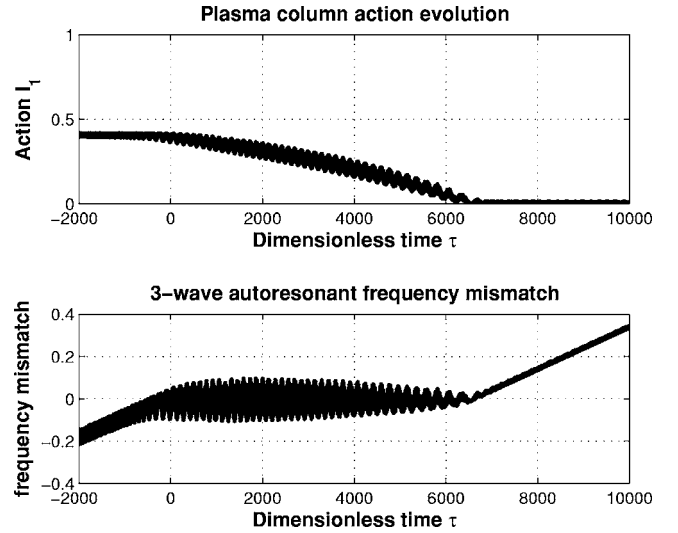

FIG. 5. Three-wave-type autoresonance for a negatively chirped frequency modulation and parameters above threshold. The diocotron mode is driven to the center of the trap. The frequency mismatch shows that the autoresonantly driven diocotron mode tracks, on average, the circuit frequency.

initial excitation $I_{10} = 0.4$ (the circuit is not excited initially). From Eq. (64), we expect the threshold value of the product $(\epsilon\delta)_{th} = 4\cdot10^{-4}$; this is in good agreement with the numerical result $(\epsilon\delta)_{num} = 4.4\cdot10^{-4}$. A modulation parameter $\delta = 0.09$ was used for this numerical analysis. The diocotron mode action and the frequency mismatch from the autoresonant condition $\dot{\Theta} - \dot{\Psi} \approx -\dot{\Theta}_c$ are plotted as a function of normalized time, with a negative chirp just above threshold, in Fig. 5. As expected, the mode action decreases and the plasma is driven towards the axis.

Now we apply a positive chirp rate using the same parameters as in the previous example. In this case, the system passes through resonance corresponding to the lower sign in Eq. (62). The numerical threshold for $\alpha = 10^{-4}$, $\Omega_c = 3.2$, $\delta = 0.04$, and $I_{10} = 0.4$ appeared to be $\epsilon_{num} = 0.0105$, which is close to the theoretical prediction, $\epsilon_{th} = 0.011$. Figure 6 shows the evolution of the system just above this threshold and, as expected, the diocotron mode is driven towards the wall of the trap. However, the evolution becomes unstable prior to reaching the wall. We have identified this effect as a Mathieu-like instability. It occurs when the coefficient $\delta\cos\Psi$ in Eq. (48) is modulated at twice the resonance frequency, $\Omega_\Psi = 2\Omega_c$. In this case, the diocotron frequency reaches the value

$$\dot{\Theta} \approx \Omega_\Psi + \Omega_c = 3\Omega_c.$$

However, from the limitation $\Omega_\psi^0 > 0$ and Eq. (61), we find that $\Omega_c \lesssim 1/(1-I_{10})$. Therefore, due to the instability, one cannot exceed

$$\dot{\Theta}_{max} \approx \frac{\Omega_d}{1-I_{max}} \lesssim \frac{3\Omega_d}{1-I_{10}}.$$

The corresponding maximum value of the action of the diocotron mode is $I_{max} \lesssim (2/3) + (I_{10}/3)$ ($I_{max} = 0.8$ for the parameters used in Fig. 6). In summary, a chirped modulation
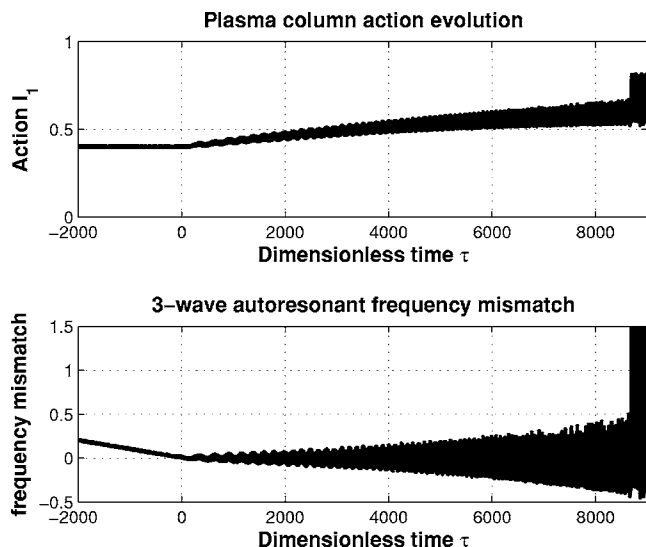
FIG. 6. Three-wave-type autoresonance for a modulation with a positively chirped frequency and parameters above threshold. The diocotron mode is driven towards the wall. A Mathieu-type instability destroys autoresonance prior to the plasma reaching the wall and the frequency tracking breaks down
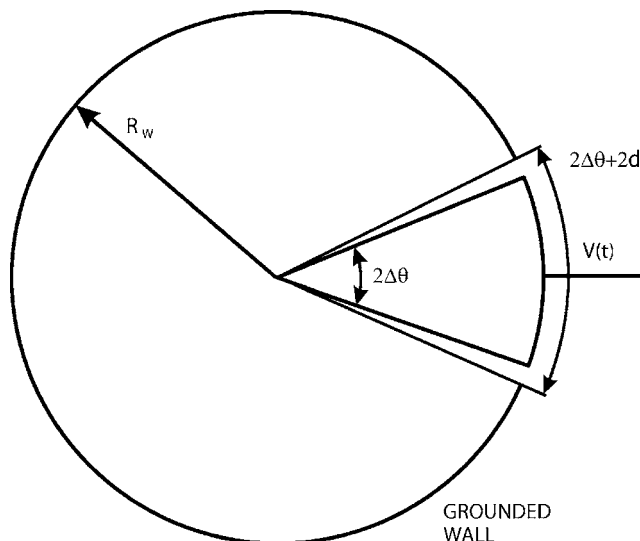

FIG. 7. A schematic of the isolated sector on the trap wall. The angular width of the sector is $-\Delta\theta < \phi < \Delta\theta$, the gaps are $-\Delta\theta - d < \phi < -\Delta\theta$ and $\Delta\theta < \phi < \Delta\theta + d$, and the length of the sector is l. In the text, it is assumed that $d \ll \theta$. A precise calculation of the electric field near the sector should include the gap effects.

of the circuit can de-excite the diocotron mode, driving the plasma towards the center of the trap, but is limited in its ability to drive the plasma to the wall.

IV. CONCLUSIONS

We have analyzed two new methods for the control of a diocotron mode. The autoresonant control methods exploit coupling with an external circuit. The external circuit is initially unexcited, but must have time-dependent parameters. A pre-excited diocotron mode can be readily manipulated, moving it towards the wall of the trap or towards the axis without feedback. An LC circuit with a swept resonant frequency drives the plasma towards the wall. Coupling to an LC circuit with a sinusoidal, chirped frequency modulation leads to a three-wave-type autoresonance and can be used to manipulate the plasma towards the center of the trap. An expression for the maximum radius that can be reached if one tries to move the plasma towards the wall via three-wave autoresonance was derived. Analytical expressions for the threshold coupling parameter required for these autoresonance schemes are found to be in good agreement with simulations. Finally, these new autoresonant control concepts may have applications to other dynamical and extended systems.

ACKNOWLEDGMENTS

APPENDIX: THE DRIVING POTENTIAL

Consider an infinite line of charge parallel to the axis of a grounded perfectly conducting cylinder of radius R_w and located (D, Θ). $D = 0$ is the center of the cylinder. From the method of images, the potential in the cylinder from the line charge is given by

$$\Phi_\lambda(r, \phi) = \frac{\lambda}{2\pi\epsilon_0} \ln\left(\frac{\sqrt{D^2 + r^2 - 2Dr\cos(\Theta - \phi)}}{\sqrt{R_w^2 + \frac{r^2 D^2}{R_w^2} - 2rD\cos(\Theta - \phi)}} \right),$$

(A1)

where λ is the charge per unit length. We are interested in the coupling to a sector patch of axial length $l \gg R_w$, so that end effects can be ignored. A schematic is in Fig. 7. The normal component of the electric field determines the total charge on the sector, located in the angular (ϕ) range of $[-\Delta\theta, \Delta\theta]$,

$$Q_\lambda = -\ \epsilon_0 l R_w \int_{-\Delta\theta}^{\Delta\theta} d\phi \left. \frac{\partial \Phi_\lambda(r, \phi)}{\partial r} \right|_{r=R_w}.$$

(A2)

With $\psi = \Theta - \phi$,

$$Q_\lambda = \frac{\lambda l (R_w^2 - D^2)}{4\pi R_w D} \int_{\Theta + \Delta\theta}^{\Theta - \Delta\theta} d\psi \frac{1}{\frac{R_w^2 + D^2}{2R_w D} - \cos(\psi)}.$$

(A3)

This integral can be easily calculated by substituting $u = \tan(\psi/2)$,

$$Q_\lambda = \frac{l\lambda}{\pi} \arctan\left[\frac{1 + D/R_w}{1 - D/R_w} \tan(\psi/2) \right] \Bigg|_{\Theta + \Delta\theta}^{\Theta - \Delta\theta}.$$

As expected, the total charge on the wall is $\lim_{\Delta\theta \to \pi} Q_\lambda = -l\lambda$.

Studying possible resonant effects requires a decomposition of the image charge into a Fourier series in terms of the angular position, θ, of the column. A simple mathematical relation,

$$\frac{1-x^2}{1+x^2-2x\cos(\phi)} = 1 + 2\sum_{k=1}^{\infty} x^k \cos(k\phi),$$

allows us to make this decomposition more obvious. We find

$$Q_\lambda = -\frac{l\lambda}{\pi}\left[\Delta\theta + \sum_{k=1}^{\infty}\left(\frac{D}{R_w}\right)^k \int_{-\Delta\theta}^{\Delta\theta} d\phi\,\cos k(\Theta-\phi)\right]$$

$$= -\frac{l\lambda}{\pi}\left[\Delta\theta + \sum_{k=1}^{\infty}\left(\frac{D}{R_w}\right)^k \frac{2\cos(k\Theta)\sin(k\Delta\theta)}{k}\right]. \quad (A4)$$

The total charge on sector patch is the sum of the charge induced from the line charge (for a grounded sector) and that induced by any external voltage, $V(t)$,

$$Q_{\text{sector}} = Q_\lambda + C_{\text{eff}}V(t), \quad (A5)$$

where we introduce an effective capacitance, C_{eff}. A precise calculation of this capacitance is not needed here and requires a detailed specification of the gap between the sector and the surrounding conducting wall.

The potential $\Phi_V(r,\phi)$ inside the cylinder and felt by the plasma, induced by the sector voltage $V(t)$, is not influenced by a small gap between the sector and the rest of the grounded wall [so long as the gap is very small compared to the sector size $(2R_w\Delta\theta)$ and the plasma does not approach very near the wall]. In this case, for negligible gap size, a Fourier expansion solution of the Laplace equation gives

$$\Phi_V(r,\phi) = \frac{V}{\pi}\left[\Delta\theta + \sum_{k=1}^{\infty}\left(\frac{r}{R_w}\right)^k \frac{2\sin(k\Delta\theta)}{k}\cos(k\phi)\right].$$

$$(A6)$$

[1] L. Friedland and A. G. Shagalov, Phys. Rev. E **71**, 036206 (2005).
[2] J. Fajans and L. Friedland, Am. J. Phys. **69**, 1096 (2001). Many examples of autoresonance can be found at www.phys.huji.ac.il/~lazar.
[3] E. M. McMillan, Phys. Rev. **68**, 143 (1945); V. Veksler, J. Phys. (USSR) **9**, 153 (1945).
[4] K. S. Golovamivsky, IEEE Trans. Plasma Sci. **11**, 28 (1983).
[5] W. K. Liu, B. R. Wu, and J. M. Yuan, Phys. Rev. Lett. **75**, 1292 (1995).
[6] B. Meerson and S. Yaviv, Phys. Rev. A **44**, 3570 (1991).
[7] R. Malhotra, Astron. J. **100**, 420 (1995).
[8] R. C. Davidson, *Physics of Nonneutral Plasmas* (Addison-Wesley, New York, 1990), p. 289.
[9] D. White, J. L. Malmberg, and C. F. Driscoll, Phys. Rev. Lett. **49**, 1822 (1982).
[10] J. H. Malmberg, C. F. Driscoll, B. Beck, D. L. Eggleston, J. Fajans, K. Fine, X. P. Huang, and A. W. Hyatt, in *Non-Neutral Plasma Physics*, AIP Conf. Proc. No. 175, edited by C. W. Roberson and C. F. Driscoll (AIP, New York, 1988), p. 28.
[11] J. H. Malmberg and J. S. deGrassie, Phys. Rev. Lett. **35**, 577 (1975).
[12] J. Fajans, E. Gilson, and L. Friedland, Phys. Rev. Lett. **82**, 4444 (1999).
[13] J. Fajans, E. Gilson, and L. Friedland, Phys. Plasmas **8**, 423 (2001).